EE568 Project 4

Baris Kuseyri

June 28, 2020

Contents

1 Introduction

DW stator topologies are the major stator type used in PMSMs. This is due to their near sinusoidal MMF which yields a high main harmonic winding factor and low torque ripple. It was not until very recently that it was shown that the right choice of slot and pole combination for a FSCW stator could yield a high main harmonic winding factor which is essential to having a high average torque [**?**]

1.1 Aims & Objectives

This paper designs an electric motor (EM) to be used as a part of an hybrid electric propulsion system for Cessna 172 Skyhawk. Definition of the hybrid electric propulsion system and the corresponding EM requirements, e.g. rated power, dimensional limitations etc., are outlined in the project proposal. Several EMs with different slot/pole combinations are designed, complying the described requirements. A comparative analysis is performed on these designs, focusing on torque density and cogging torque aspects. One design is chosen, and further alterations are applied to enhance the EM performance. Additionally, this paper proposes a novel winding topology to reduce the cogging torque.

2 Literature Review

The term FSCW is used to indicate that EM has a non-integral number of slots-per-pole-per-phase q,

$$q = \frac{Q}{2pm}$$

where, Q is number of slots, $2p$ is number of poles and m is number of phase.

FSCW topologies are reported to exhibit higher power density. CW comprises of shorter end-windings, resulting with a lower copper loss due to end-windings, compared to DW. FSCW topologies display higher self-inductance, leading to a wider field-weakening region [**?**]. The aspect of fault-tolerant in an EM is proportional to several characteristics.

First of all, magnetic coupling between phases, which implies a high mutual inductance, diminishes the fault-tolerancy of an EM. Therefore, phases which are magnetically seperated is desired to achieve a higher fault-tolerancy rating [**?**]. In SPM machines, single-layer winding demonstrates higher self-inductances and lower mutual inductances compared to its double-layer counterparts. A high self-inductance limits the amplitude of short-circuit current, a significant property for fault-tolerancy [**?**] [**?**].

Secondly, it is desired to have phases which are physically seperated to achieve fault-tolerancy[**?**]. Lastly,

Mutual coupling between phasesTo achieve a greater fault-tolerant EM

Fractional-Slot Concentrated-Winding (FSCW) topology has become of great interest, since it provides a vast amount of choices for the electric motor (EM).

analytical modelling of the stator MMF and machine equivalent airgap function are essential to correct calculation of the stator magnetic field and inductances, and subsequently torque and torque ripple. analytical formulae for the stator MMF. [**?**].

2.1 Torque Density

2.2 Torque Ripple

3 torque components are present in FSCW PMSM. These are: alignment torque, reluctance torque and cogging torque.

$$T_{em}(t) = T_{align}(t) + T_{rel}(t) + T_{cog}(t)$$

Torque generated as a result of the interaction between stator and rotor MMF is alignment torque. $p/2$th harmonic of PM flux linkage, corresponding to fundamental component, contributes to the average alignment torque. Remaining harmonic components provides for the alignment torque ripple [**?**]. Torque generated as a result of the stator field aligning the rotor as the reluctance of the magnetic circuit is minimum. Reluctance varies according to the rotor position, while an IPM machine is magnetically salient. This saliency forms as the PM permeability is approximately equals to that of air; thus, contributing to the air-gap length. Similar to alignment torque, $p/2$th harmonic of self and mutual inductance, corresponding to fundamental component, contributes to the average alignment torque. Remaining harmonic components provides for the reluctance torque ripple [**?**].

Cogging torque is one of the torque elements contributing to the torque ripple in the PMSM. Several design factors lead to variation on cogging torque. Here, one such aspect is investigated, that is the amount of stator teeth aligned with poles in the rotor at a given instance. For the corresponding magnetic circuit, permeance is highest when a rotor pole and a stator tooth are aligned. This results with a force that tries to keep the pole steady; hence, emerging a torque counter to the rotor rotation. This is called 'cogging torque'. More of such alignments result with more cogging torque. This description leads to the statement that the value of least common multiple (LCM) of the number of slots Q and number of poles $2p$ is an indicator for the intesity of the cogging torque in a PMSM. LCM of Q and $2p$ is inversely proportional to the cogging torque amplitude [**?**] [**?**].

FSCW stator topologies are characterized by their slots per pole per phase ratio, denoted S_{pp}[**?**].

3 Analytical Calculation & Sizing

As mentioned in the proposal the machine rating are,

Power [kW]	Speed [rad/s]	Torque [N·m]
46.9790	282.7433	166.1542

Table 1: Lycoming Operator's Manual IO-360-L2A Operating Conditions

3.1 Magnetic Loading & Electrical Loading

Permitted RMS values for linear current densities $\bar{A}$, current densities J and peak air-gap flux densities for PMSMs with single-layer field winding, and the corresponding tangential stress σ_{Ftan} are reported as follows: Here, σ_{Ftan} is calculated by

$\bar{A}$ $[kA/m]$	$\hat{B}_g$ $[T]$	J $[A/mm^2]$	σ_{Ftan} $[Pa]$
35-65	0.85-1.05	2-4	21000-48000
50	0.95		33876

Table 2: PMSMs with Single-Layer Field Winding

$$\sigma_{Ftan} = \frac{\hat{A}\hat{B}_g}{2} = \frac{\bar{A}\hat{B}_g}{\sqrt{2}} \tag{1}$$

where, $(\hat{\cdot})$ is for peak value and $(\bar{\cdot})$ is for RMS value of the parameter. Therefore, suitable magnetic and electric loading are chosen as

3.2 Specific Machine Constant

$$\begin{aligned} C &= \frac{\pi^2}{\sqrt{2}} k_w \bar{A}\hat{B}_g = \frac{\pi^2}{2} k_w \hat{A}\hat{B}_g \\ &= \frac{\pi^2}{\sqrt{2}} k_w \cdot 50 \cdot 0.95 \\ &= 331496.1 \cdot k_w [W/m^3] \end{aligned}$$

where, k_w is the winding factor.

3.3 Rough Dimensions

Rotor Volume V_r in PMSMs can be calculated in a similar manner with asynchronous machines

$$\begin{aligned} T &= \sigma_{Ftan} r_r (2\pi r_r l') \\ &= \sigma_{Ftan} V_r \end{aligned}$$

$$\begin{aligned} V_r &= \pi \frac{D_r^2}{2} l' = \frac{T}{2\sigma_{Ftan}} \\ &= \frac{166.1542}{2 \cdot 33876} = 0.0025 [m^3] \end{aligned}$$

Air-gap Clearance in PMSMs can be calculated in a similar manner with asynchronous machines

$$\begin{aligned} \delta_g &= \frac{0.18 + 0.006P^{0.4}}{1000} [m] = \frac{0.18 + 0.006 \cdot 46979^{0.4}}{1000} [m] \\ &= 6.235195394489506e - 04 [m] \\ &\approx 0.624 [mm] \end{aligned}$$

Equivalent Machine Length to Air-gap Diameter $\chi = \frac{l'}{D_g}$ in synchronous machines with pole-pair number more than 1, i.e. $p > 1$, this ratio is calculated as

$$\chi = \frac{l'}{D_g} \approx \frac{\pi}{4p}\sqrt{p}$$

where, the p stands for number of pole pairs in the machine. χ ratio for different number of pole-pairs p can be seen in Fig. 1.

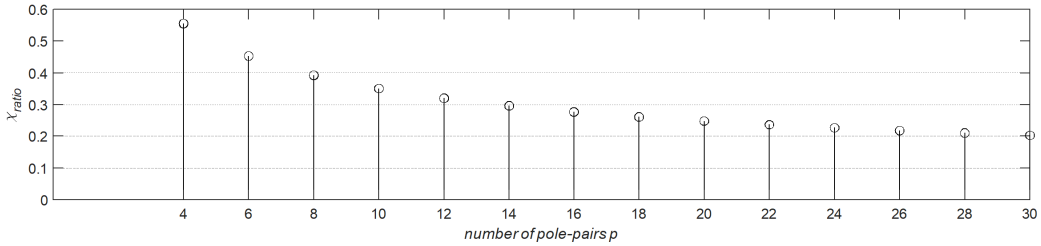

Figure 1: χ ratio for different number of pole-pairs p

airgap clearance	0.7mm
rotor diameter	290mm
axial length	68mm

Table 3: Rough Dimensions

3.4 Winding Configurations

This paper analyses single-layer FSCW winding configurations. In this manner, topologies with number of slots as $Q = 18, 24$, and number of poles as $2p = 16, 20, 22, 26, 28$ are inspected. These slot/pole combinations and their corresponding winding factors are presented in Table 4.

$Q/2p$	16	20	22	26	28
18	0.945	0.945	0.902	0.735	0.617
24	0.866	0.966	0.958	0.958	0.966

Table 4: Winding Configurations

3.5 Machine Parameters

Split Ratio λ is the ratio of rotor outer diameter to stator outer diameter $s = D_{ro}/D_{so}$. Wu et al. derives the optimal split ratio for IPM machines with non-overlapping windings using torque

number of slots
number of coils
cable size

Table 5: Winding Configurations

density equation [**?**]. First, a flux density ratio γ is defined as the ratio of air-gap flux density to maximum flux density the stator lamination can support before magnetically saturating. Split ratio λ, flux density ratio γ and another intermediary ratio k is defined in 2. The expression derived for the optimal split ratio is

$$B_g = \frac{3\sqrt{3}}{2\pi} B_{gmax}$$

$$\lambda = \frac{D_{ro}}{D_s o} \qquad \gamma = \frac{B_g}{B_{max}} \qquad k = \frac{p}{Q} \tag{2}$$

where, D_{ro} is rotor outer diameter, D_{so} is stator outer diameter, B_g is the average airgap flux density, p is the number of pole-pairs and Q is the number of slots. Then, the optimal split ratio expression is derived as

$$\lambda = \frac{-b_1 - \sqrt{b_1^2 - 4a_1}}{2a_1}$$

$$a_1 = 2\big[\frac{k\pi}{p}(\frac{k\pi}{p} + 2)\gamma^2 + 2\gamma - 1\big] \qquad b_1 = -3(\frac{k\pi}{p} + 1)\gamma$$

teeth/slot opening this paper utilizes parallel teeth topology with a slot opening to tooth width ratio of 50:50. This means that at the inner side of the stator, the section on the stator retained for one slot and one tooth is divided equally between those two. Therefore, the tooth width is

$$\tau_{tooth,i} = \tau_{tooth,o} = \frac{\pi D_{si}}{2Q} = \tau_{tooth} = \tau_{slot,inner} \tag{3}$$

where, D_{si} is the stator inner diameter.

back-core thickness are set to be equal to the tooth width of the EMs. In single-layer FSCW topologies, phases are magnetically decoupled, meaning that the flux runs through coupled adjacent poles. Therefore, the flux travels through one tooth continues its path through the back iron to the adjacent tooth and the corresponding pole, without interacting with other flux paths at the back iron. Therefore, back-iron thickness doesn't have to be higher than the tooth thickness.

$$h_{back-iron} = \tau_{tooth} \tag{4}$$

teeth/slot height can be calculated by

$$h_{tooth} = h_{slot} = \frac{D_{so}}{2} - h_{back-iron} - \frac{D_{ro}}{2} - \delta_g \tag{5}$$

slot outer length can be calculated by

$$\tau_{slot,outer} = \frac{\pi(D_{so} - 2h_{back-iron})}{Q} - \tau_{tooth} \tag{6}$$

back-core thickness	19.07mm
number of coils	
cable size	

Table 6: Machine Parameters

3.6 Material selection

Magnet Material There are no cost limitations to the EM application. Eclipse Magnetics inform that N35 grade NdFeB magnets have the VH/AH choice, in which the magnet can operate up until the temperatures of $230°C$. This is not a requirement for the application, however, implementing N35 PM magnets omits the machine's operable temperature range dependency to the PM magnet demagnetization due to heat. N35 grade NdFeB magnet characteristics are given in Table. 7

B_r $[mT]$	H_c $[kA/m]$	Max. Energy BHMax $[kJ/m^3]$
1170	867	263

Table 7: N35 grade NdFeB PM characteristics

where, B_r is remanence flux density and H_c is coercivity.

back-core thickness	19.07mm
number of coils	
cable size	

Table 8: Material selection

Lamination Material

3.7 Electrical circuit parameter

3.8 Overall

number of coils cable size

4 FEA Modelling

5 Comparison & Discussion

6 Conclusion

7 Draft

1[?] 2[?] 3[?] 4[?] 5[?] 6[?] 7[?] 8[?] 9[?] 10[?] 11[?] 12[?] 13[?] 14[?] 15[?] 16[?] 17[?] 18[?] 19[?] 20[?] 21[?] 22[?] 23[?] 24[?]

$Q = 18$	$p = 16$	$p = 20$	$p = 22$	$p = 26$	$p = 28$
Magnetic Loading $\hat{B}[T]$	0.95				
Electric Loading $\hat{A}[A/m]$	50000				
Tangential Stress $\sigma_{Ftan}[Pa]$	33876				
Rotor Volume $V_r[m^2]$	0.002473447965892				
Air-gap Clearance $\delta_g[mm]$	0.624				
Linear Current Density $J[A/mm^2]$	3.27	3.15	3.10	3.02	2.98
Specific Machine Constant	313264	313264	299009	243650	204533
Axial Length $l[mm]$	49.6	46.1	44.6	42.2	41.2
Winding Factor k_w	0.945	0.945	0.902	0.735	0.6170
Rotor outer diameter $D_{ro}[mm]$	252.2	261.7	265.9	273.4	276.8
Stator inner diameter $D_{si}[mm]$	253.4	263.0	267.2	274.7	278.1
Stator outer diameter $D_{so}[mm]$	398.5	413.6	420.2	432.1	437.4
Tooth width $\tau_{teeth}[mm]$ Slot inner width $\tau_{slot,inner}[mm]$ back-iron thickness $h_{back-iron}[mm]$ Tooth height $h_{teeth}[mm]$ Slot heigth $h_{teeth}[mm]$	22.0	22.8	23.2	23.9	24.2
Slot outer width $\tau_{slot,outer}[mm]$	50.5	52.5	53.3	54.8	55.5
$Q = 24$	$p = 16$	$p = 20$	$p = 22$	$p = 26$	$p = 28$
Linear Current Density $J[A/mm^2]$	3.96	3.81	3.75	3.65	2.60
Specific Machine Constant	287076	320225	317573	317573	320225
Axial Length $l[mm]$	49.6	46.1	44.6	42.2	41.2
Winding Factor k_w	0.866	0.966	0.958	0.958	0.966
Rotor outer diameter $D_{ro}[mm]$	252.2	261.7	265.9	273.4	276.8
Stator inner diameter $D_{si}[mm]$	253.4	263.0	267.2	274.7	278.1
Stator outer diameter $D_{so}[mm]$	391.5	406.3	412.8	424.5	429.8
Tooth width $\tau_{teeth}[mm]$ Slot inner width $\tau_{slot,inner}[mm]$ back-iron thickness $h_{back-iron}[mm]$ Tooth height $h_{teeth}[mm]$ Slot heigth $h_{teeth}[mm]$	16.5	17.1	17.4	17.9	18.1
Slot outer width $\tau_{slot,outer}[mm]$	52.5	54.5	55.4	57.0	57.7
	29.9	31.0	31.5	32.4	32.8

Table 9: Machine Parameters